THE JOURNAL OF PHYSICAL CHEMISTRY A

Article

pubs.acs.org/JPCA

Vibrational Energy Flow between Modes by Dynamic Mode Coupling in THIATS J-Aggregates

Daisuke Hasegawa,[†] Kazuaki Nakata,[†] Eiji Tokunaga,[†] Kotaro Okamura,[‡,§] Juan Du,[‡,§] and Takayoshi Kobayashi*[,‡,§,∥,⊥]

[†]Department of Physics, Faculty of Science, Tokyo University of Science, 1-3 Kagurazaka, Shinjuku, Tokyo 162-8601, Japan

[‡]Department of Applied Physics and Chemistry and Institute for Laser Science, University of Electro-Communications, 1-5-1 Chofugaoka, Chofu, Tokyo 182-8585, Japan

[§]Core Research for Evolutional Science and Technology (CREST), Japan Science and Technology Agency, K's Gobancho, 7, Gobancho, Chiyoda-ku, Tokyo 102-0076, Japan

[∥]Department of Electrophysics, National Chiao-Tung University, Hsinchu 300, Taiwan

[⊥]Institute of Laser Engineering, Osaka University, 2-6 Yamada-oka, Suita, Osaka 565-0971, Japan

ABSTRACT: We performed ultrafast pump−probe spectroscopy of J-aggregates of 3,3′-disulfopropyl-5,5′-dichloro-9-ethyl thiacarbocyanine triethylammonium (THIATS), one of the most typical cyanine dyes, and detected excited molecular vibrations, using a sub-10 fs pulse laser. The time-resolved two-dimensional difference absorption (ΔA) spectra are observed between −314 and 1267 fs. By performing the Fourier transform and spectrogram analysis, vibrational modes in THIATS are observed at 285, 485, 555, 824, and 1633 cm^{-1} and there was a modulation of the vibrational frequencies around 1633 cm^{-1} which depend on the delay time, respectively. By the analysis of the modulation, energy flow is found to take place from other modes to the 1633 cm^{-1} mode through the low frequency mode with ∼50 cm^{-1}. Also, by fitting the real-time traces of ΔA with the sum of two exponential functions and a constant term, the average lifetimes of three electronically excited states were found to be τ_1 = 52 ± 5 fs and τ_2 = 540 ± 78 fs. By performing single-exponential fitting around the stationary absorption peak at 1.990 eV, in the negative time range, the electronic dephasing time, T_2^{ele}, is determined to be 18.30 fs.

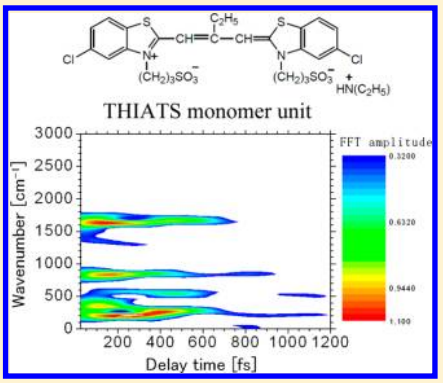

INTRODUCTION

Some kinds of dye molecules dissolved in solution with concentration exceeding a certain level form J-aggregates, nanostructures with sizes intermediate between molecular crystals and isolated molecules.[1−7] J-aggregates have been extensively studied both experimentally and theoretically as a model material for one-dimensional Frenkel excitons.[8,9] J-aggregates are characterized by the sharp excitonic absorption peak called the J-band, red-shifted from the monomer band, exhibiting a remarkable optical response.[10,11] For example, it is reported that the formation of J-aggregates enhances the electrooptic Kerr effect by 10^2 times compared with that of the monomer molecules.[12] These optical properties of J-aggregates have been attracting great interest in both fields of chemistry and physics.[13] However, it has yet to be determined how the structures of J-aggregates are correlated to their electronically excited states because of very weak exciton−phonon (intramolecular vibration) coupling in the Frenkel excitons of the J-aggregates. In fact, coherent molecular vibrations induced by electronic (excitonic) excitation have been observed only for aggregates of pseudoisocyanine (PIC)[14] and tetraphenylporphine tetrasulfonic acid (TPPS).[15−17]

J-aggregates of cyanine dyes are promising for future applications to photoelectric cells and nonlinear optical devices.[18] The photophysical properties including the temperature dependence of the J-aggregates of THIATS in various aqueous solvents, which is classified as a kind of cyanine dye, have been studied by time-resolved fluorescence measurements.[19−26]

However, time-resolved absorption dynamics, molecular vibration properties, and Raman spectra of THIATS have not yet been studied. It is therefore interesting to apply time-resolved impulsive stimulated Raman scattering measurements to this molecular aggregate system.

In the present work, using a sub-10 fs ultrashort pulsed laser, we have performed time-resolved pump−probe spectroscopy of J-aggregates of THIATS and have studied extensively the dynamics of impulsively pumped coherent molecular vibrations. As a result, the particular vibrational modes, lifetimes, frequency modulation observed by spectrogram, and electronic dephasing time of J-aggregates of THIATS are obtained.

Received: February 12, 2013
Revised: October 9, 2013
Published: October 10, 2013

dx.doi.org/10.1021/jp4015228 | J. Phys. Chem. A 2013, 117, 11441−11448

EXPERIMENTAL METHODS

Materials. 3,3′-Disulfopropyl-5,5′-dichloro-9-ethyl thiacarbocyanine triethylammonium (THIATS, Hayashibara, Okayama, Japan) and polyvinyl alcohol (PVA, Wako Pure Chemical, Osaka, Japan) were used without further purification. The molecular weight of THIATS is 750.82.

Preparation of Sample Films. THIATS (8 mg) and PVA (80 mg) were dissolved in 2 mL of distilled water stirring at 120 °C ensuring complete dissolution.[7] A thin film of THIATS J-aggregates was formed by spin coating on a glass substrate (76 × 26 × 1 mm^3).[27] Figure 1 shows the stationary absorption

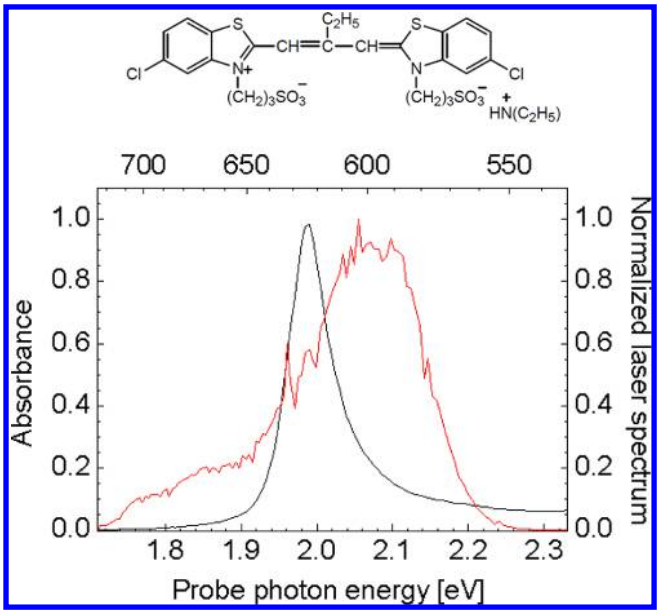

Figure 1. The chemical structure of the THIATS monomer (top), the stationary absorbance (black line), and the laser spectrum (red line). The stationary absorption spectrum of the formed THIATS J-aggregate films was recorded using a spectrophotometer (UV-3101PC; Shimadzu) at a constant temperature (293 K). The laser spectrum was recorded using the combination of a polychromator and a multichannel lock-in amplifier.

spectrum of the formed THIATS J-aggregate films recorded using a spectrophotometer (UV-3101PC; Shimadzu) at 293 K. The absorption spectrum of THIATS J-aggregates has a peak at 1.990 eV. The full width at half-maximum (fwhm) of the stationary absorbance is 0.0684 eV.

Real-Time Pump−Probe Experimental Apparatus. The pulsed source for the pump−probe experiment is the noncollinear optical parametric amplifier (NOPA) described elsewhere.[28−32] Briefly, the NOPA system was pumped with a commercially supplied regenerative amplifier (Spectra Physics, Spitfire). The output of the NOPA seeded with a white-light continuum was compressed to sub 10 fs. The output spectral range extended from 532 to 725 nm, indicating that the pulses were nearly Fourier-transform-limited. Both pump and probe pulses were generated from the NOPA. The pulse duration was about 10 fs at the inner surface of the sample cell window. The pulse energies of the pump and probe were typically about 42 and 6 nJ, respectively.

Pump−probe spectral data were detected by the combined system of a polychromator and a multichannel lock-in amplifier to detect the pump−probe signal.[33] After the sample, the probe pulses were dispersed by the polychromator (300 grooves/mm, 500 nm blazed) and guided simultaneously to the 128 avalanche photodiodes by a 128-channel bundle fiber.

Figure 1 shows the laser spectrum. The peak energy and the fwhm of the laser spectrum were about 2.1 and 0.19 eV, respectively. Here, the laser spectrum covers the entire region of the stationary absorption spectrum. The spectral resolution of the total system is about 1.5 nm. The wavelength dependent difference absorbance of the probe at 128 wavelengths was measured by changing the pump−probe delay times from −314 to 1267 fs with a 1.1 fs step. All the experiment was performed at a constant temperature (293 K).

RESULTS AND DISCUSSION

Vibrational Frequencies Observed in the Pump−Probe Spectral Data. The time-resolved two-dimensional (2D) Δ*A* spectra of PVA films measured with the 10 fs pump−probe system is shown in Figure 2 in the above. Red - yellow -

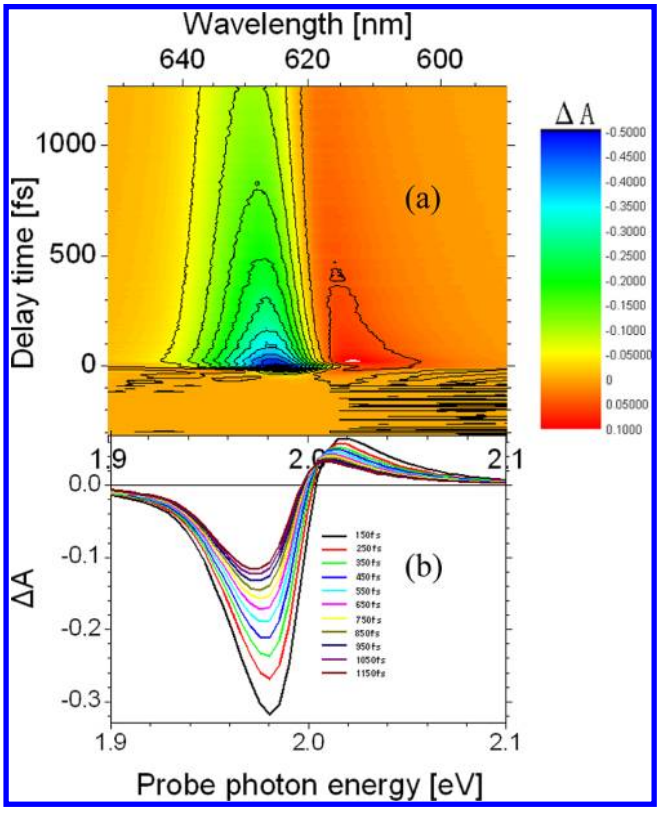

Figure 2. (a) Time-resolved two-dimensional (2D) difference absorption spectra. Δ*A* was measured with the 10 fs pump−probe system. Red - yellow - blue color tones indicate positive Δ*A* (increase) and negative Δ*A* (decrease) changes. (b) Averaged, for 100 fs, absorbance change spectra at delay times of 150 (black line), 250 (red line), 350 (green line), 450 (blue line), 550 (cyan line), 650 (pink line), 750 (yellow line), 850 (dark yellow line), 950 (navy line), 1050 (purple line), and 1150 (wine line) fs.

blue color tones indicate positive Δ*A* (increase) and negative Δ*A* (decrease) changes. Figure 3 shows Δ*A* traces at four representative probe photon energies. The time traces contain a slow decay and rapid oscillations reflecting the electronic relaxation and vibration dynamics, respectively. Exponential fitting to the observed ultrafast dynamics of the THIATS J-aggregates is shown in Figure 3. The bottom of Figure 2 shows the time-resolved Δ*A* spectra averaged for 100 fs at the central delay times between 150 and 1150 fs with a 100 fs step. The

dx.doi.org/10.1021/jp4015228 | J. Phys. Chem. A 2013, 117, 11441−11448

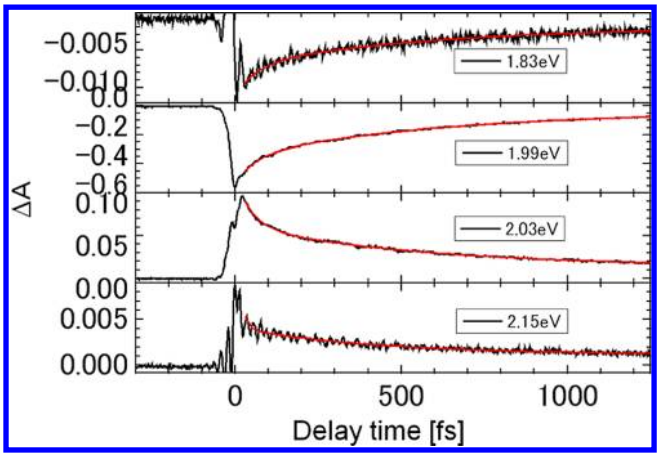

Figure 3. Real-time traces of ΔA at 1.83, 1.99, 2.03, and 2.15 eV (black line) and the two exponential functions which were fitted to the real-time traces of ΔA (red line).

ΔA is negative and becomes positive in the lower and higher probe photon energy region than about 2.0 eV. The positive ΔA signal is due to the induced absorption from the n ($\geq$1) exciton state to the (n + 1) exciton state.[8] The negative ΔA signal is due to the mixed contributions of the stimulated emission from the n ($\geq$1) exciton state to the (n − 1) exciton state and the ground-state depletion. The negative and positive ΔA peaks and the probe photon energy of null difference absorbance "ΔA = 0" shift gradually toward the lower photon energy with the elapsed time.

To discuss the oscillatory signals, fast Fourier transformation (FFT) was performed on the real-time vibrational traces from delay times of 107−1267 fs using a Hanning window function covering the full positive measurement range. The nonzero starting delay time for this analysis is because of interference between the scattered pump and the probe pulses in the vicinity of the zero delay time.[14] The results of FFT are shown two-dimensionally in Figure 4. The wavenumber resolution is 7.7 cm^{-1} determined by the condition of FFT: The time trace taken with a 1.055 fs step, corresponding to the full span of the Fourier spectrum, is the inverse of the temporal step, 31595 cm^{-1}. This is divided by 4096 data points in the FT spectra to obtain 7.7 cm^{-1}. Along a vertical cross section at 1.970 eV in the 2D FFT amplitude spectra shown in Figure 4, there are five prominent peaks at 262, 485, 547, 824, and 1633 cm^{-1}.

Determination of Time Constants. In a previous paper from our group, Minoshima et al. explained experimental results by assuming that J-aggregates of a cyanine dye have four electronic states (n ($\geq$3)-exciton state, 2-exciton state, 1-exciton state, and the ground state) and discussed the dynamics in detail.[8] Here, just as in this case, the authors assumed that the excited THIATS has four electronic states. Then, to determine the time constants of the above processes, the real-time traces of ΔA in the time region between 31 and 1267 fs were fitted with the sum of two exponential functions and a constant term from 1.72 to 2.34 eV. The probe photon energy dependences of the two relaxation time constants, τ_1 and τ_2, determined by two exponential fitting function are shown in Figures 5 and 6, respectively. The reliability of the time constants in the probe photon energy regions below 1.924 eV and above 2.103 eV is lower than that in the region 1.924−2.103 eV because of the smaller ΔA signal in the former. Therefore, the lifetimes, τ_1 and τ_2, determined by averaging in this reliability of range are 52 ± 5 and 540 ± 78 fs, respectively. Here, the data between 2.013 and 2.020 eV are also excluded, because the ΔA signal in this region is very small.

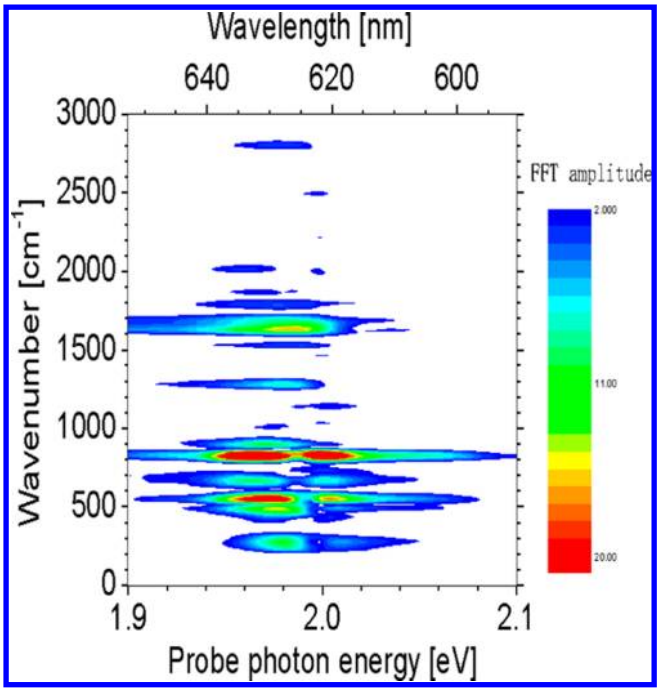

Figure 4. Two-dimensional (2D) FFT amplitude spectrum. FFT was performed on the real-time vibrational traces from a delay time of 107 to 1267 fs using a Hanning window function. The wavenumber resolution is 7.7 cm^{-1} determined by the condition of FFT. In order to remove a large DC background, a high-pass filter with a cutoff frequency of 150 cm^{-1} is used for FFT.

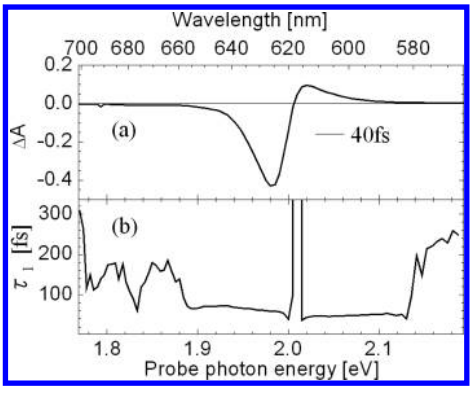

Figure 5. (a) ΔA spectra at a delay time of 40 fs. (b) Dependence of time constants τ_1 on the probe photon energy, obtained by fitting with the two exponential functions.

ΔA spectra in Figure 2 show a time-dependent red-shift of the zero cross point, demonstrating multiexciton contributions, i.e., sequential decay from n-exciton to (n − 1) exciton states. The decay kinetics in Figures 2 and 3 consist of long decay components (>10 ps) due to the 1-exciton state and the ground state depletion + fast decay components (~540 fs) due to the 2-exciton states + fastest decay components (~52 fs) due to the 3-exciton states. The ground state depletion (>100 ps) gives the main absorption decrease peak at 1.98 eV, corresponding to the stationary absorption spectrum. The 1-exciton state observed in the time range >10 ps gives a decrease in the absorption intensity due to induced emission from the 1-

dx.doi.org/10.1021/jp4015228 | J. Phys. Chem. A 2013, 117, 11441−11448

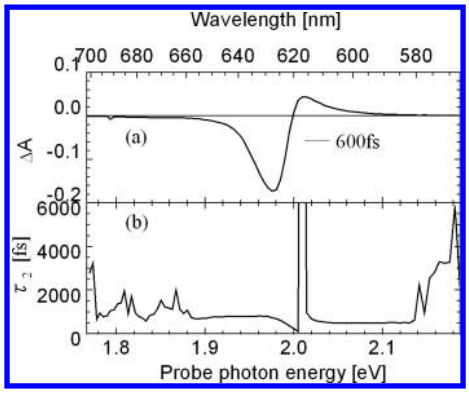

Figure 6. (a) ΔA spectra at a delay time of 600 fs. (b) Dependence of time constants τ_2 on the probe photon energy, obtained by fitting with the two exponential functions.

exciton state to the ground state and an increase due to 1- to 2-exciton induced absorption at almost the same weight. The 2-exciton state with ~540 fs lifetime shows a blue-shifted decrease in absorption intensity due to 2- to 1-exciton induced emission and blue-shifted increase due to 2- to 3-exciton induced absorption at almost the same weight. The 3-exciton state with 52 fs lifetime gives a further blue-shifted absorption decrease due to 3- to 2-exciton induced emission and further blue-shifted absorption increase due to 3- to 4-exciton induced absorption at almost the same weight. Since the 1-, 2-, and 3-exciton contributions are substantially overlapping with each other being associated with a slight blue shift, they hence show almost similar kinetics over the whole ΔA spectra in Figures 5 and 6 with slightly shorter decay time for ΔA increase than for ΔA decrease.

Here, we did not intend to clarify multiexciton dynamics but made a phenomenological fit to obtain the typical time scale for the decay. Spectral overlaps of respective contributions of n-exciton states make the analysis difficult. Although a rigorous analysis of the multiexciton dynamics is difficult, we show a significant role of exciton−exciton annihilation in the observed fast decay dynamics in the Appendix.

Spectrogram Analysis. The time-dependent shifts of wavenumber of the relevant vibration were analyzed using spectrogram, which is a time-gated Fourier transform.[34] The spectrogram shown in Figure 7 was calculated by applying a sliding-gate Fourier transform to the ΔA traces averaged over

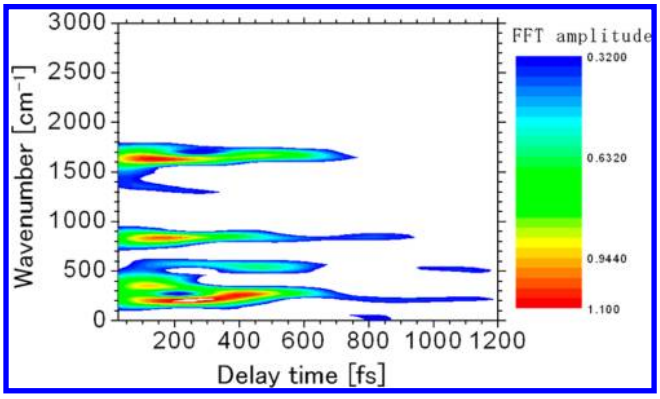

Figure 7. Spectrogram. The spectrogram trace was calculated by shifting the window at a 1 fs step in the delay time. The wavenumber resolution of the spectrogram is 27 cm^{-1}.

the probe energies from 1.902 to 1.995 eV. A Blackman window function with a full width at half-maximum of 740 fs was used in the spectrogram analysis. The spectrogram trace was calculated by shifting the window at 1 fs step along the delay time. The wavenumber resolution of the spectrogram is 27 cm^{-1}. The data in the vicinity of the zero delay is disturbed by the interference between the scattered pump and the probe pulses. In the time-resolved vibrational spectrum of THIATS J-aggregates (Figure 7), vibrational bands appeared around 1633 cm^{-1} just after photoexcitation. Additionally, as can be seen in Figure 7, there are many modulations of the vibrational frequencies which depend on the delay time.

Parts a and b of Figure 8 show the time dependence of the vibrational frequency at the FFT amplitude peak (frequency modulation) and the vibrational value of the FFT amplitude (amplitude modulation) around 1633 cm^{-1}. Here, the wavenumber at the FFT amplitude peak and values of FFT amplitude were determined by a polynomial function fitted with the FFT amplitude of cross section of the spectrogram.

In our previous studies, time dependent vibrational mode coupling, which we called dynamic mode coupling, was discussed using spectrograms.[35−37] To discuss the modulation of vibrational wavenumber, FFT was performed for the instantaneous frequency modulation and amplitude modulation obtained by the spectrogram analysis around 1633 cm^{-1}, using the Hanning window function (Figure 8d and e). Parts d and e of Figure 8 show that the 1633 cm^{-1} mode has the amplitude modulation and frequency modulation with a modulation frequency of 49 ± 19 and 61 ± 20 cm^{-1}, respectively. These two are close enough to each other to conclude that the amplitude and frequency modulation are coupled to each other. The initial phases of the frequency modulation and amplitude modulation of the 1633 cm^{-1} mode are 0.92π and 0.96π, respectively. Both of the values are close to π, indicating that the coupling with the other mode is modulated in a synchronously coupled manner with a low wavenumber of 50−60 cm^{-1}.

Since the frequency modulation and the amplitude modulation are nearly in phase, as shown in the spectrogram analysis, the concomitant increase in spring constant and amplitude apparently does not satisfy energy conservation within this single mode. Thus, if the law is satisfied within the 1633 cm^{-1} mode, the frequency modulation and amplitude modulation of the 1633 cm^{-1} mode should be antiphase with respect to each other.[38] Instead, the in-phase behavior indicates that energy flow is taking place from other modes to the 1633 cm^{-1} mode through the low frequency mode of 50−60 cm^{-1}.

Then, let us discuss the 824 cm^{-1} mode. In the same way as described above, FFT was performed for the 824 cm^{-1} mode (Figure 9). This mode also has the amplitude modulation and frequency modulation with the modulation frequency of 59 ± 21 cm^{-1} (Figure 9c and e) and 63 ± 22 cm^{-1} (Figure 9a and d). Here, FFT was performed on the time dependence of ΔA averaged from 1.902 to 1.995 eV for the delay times from 20 to 1267 fs using a Hanning window function, because the data in the vicinity of the zero delay was disturbed by the interference between the scattered pump and probe pulses. As Figure 10 provides, there is a prominent peak in the FFT amplitude spectrum at a wavenumber of 49 ± 19 cm^{-1}, in good agreement with the low frequency modulation of 50−60 cm^{-1}.

There are two candidates of the very low frequency mode with 49 ± 19 cm^{-1}. One is the vibration mode which changes the molecular structure due to out-of-plane deformation

dx.doi.org/10.1021/jp4015228 | J. Phys. Chem. A 2013, 117, 11441−11448

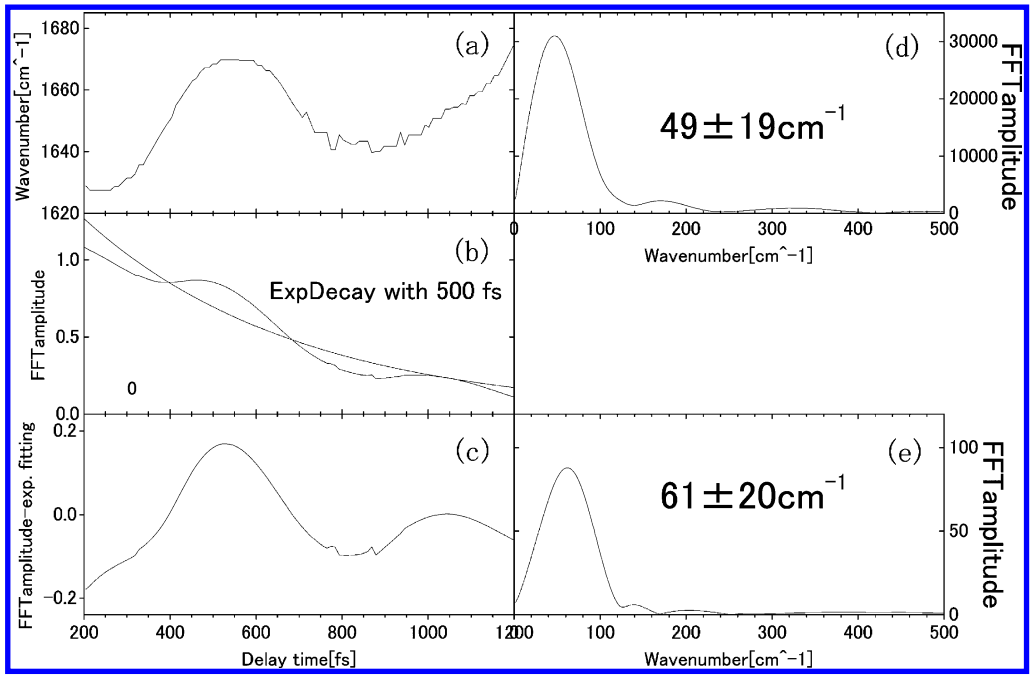

Figure 8. (a) Time dependence of frequency modulation around 1633 cm^{-1}. (b) Time dependence of amplitude modulation, fitted with the exponential decay curve with a decay time of 500 fs. (c) Difference calculated by subtracting the exponential decay curve from the amplitude modulation. (d) FFT amplitude spectrum of the frequency modulation in part a. (e) FFT amplitude spectrum of the amplitude modulation in part c.

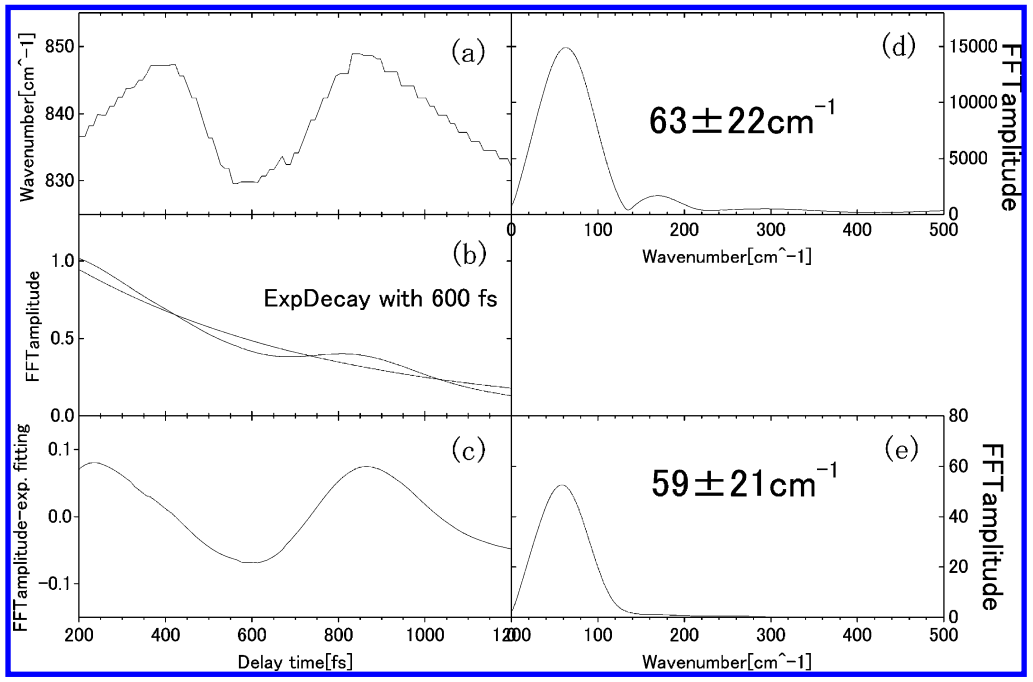

Figure 9. (a) Time dependence of frequency modulation around 824 cm^{-1}. (b) Time dependence of amplitude modulation. fitted with the exponential decay curve with a decay time of 600 fs. (c) Difference calculated by subtracting the exponential decay curve from the amplitude modulation. (d) FFT amplitude spectrum of the frequency modulation in part a. (e) FFT amplitude spectrum of the amplitude modulation in part c.

extending to the full size of the molecule, resulting in the mixing between the 824 and 1633 cm^{-1} modes. The latter is a C−C stretching mode, and the former is probably an out-of-plane C−C−C bending mode attached to the phenyl ring.

The other candidate is an intermolecular vibrational mode. In the discussions so far, the very low frequency modes are thought of as out-of-plane vibration in ref 39. However, the ∼50 cm^{-1} mode obtained in the present study is much lower than the very low frequency mode which was referred to in ref 39. Therefore, the very low frequency mode can be a phonon mode (one-dimensional lattice vibration mode). Then, by considering the phonon frequency of typical crystalline BN (molecular weight: 24.82) and SiC (molecular weight: 40.10), the maximum phonon frequency of THIATS is estimated. As a result, the maximum phonon frequency of THIATS is 118−165 cm^{-1}.[40,41] Here, it is assumed that the bonding strength in J-aggregates due to static electric force is not greater than that in BN and SiC due to a covalent bond. Since the frequencies

dx.doi.org/10.1021/jp4015228 | J. Phys. Chem. A 2013, 117, 11441−11448

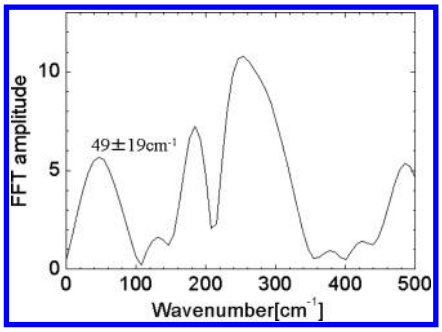

Figure 10. FFT amplitude spectrum. FFT was performed on the real-time vibrational traces, where the exponential decay component was subtracted from the average between 1.938 and 2.00 eV from a delay time of 107−1267 fs in Figure 2, using a Hanning window function. The wavenumber resolution is 7.7 cm^{-1} determined by the time range of FFT.

estimated from the molecular weight of 750.82 for THIATS, which is considered to form a lattice unit, are much lower than those of BN and SiC, the low frequency mode can be an intermolecular vibration mode.

Electronic Dephasing Time. Electronic coherence in the sample with the duration of electronic dephasing time is generated by the probe pulse.[42]

By performing a single-exponential fit around the stationary absorption peak (1.990 eV) in the time region between −314 and −1.1 fs to avoid interference between the scattered pump and probe pulses in the vicinity of the zero delay time, as you see from Figure 11, the electronic dephasing time is obtained.

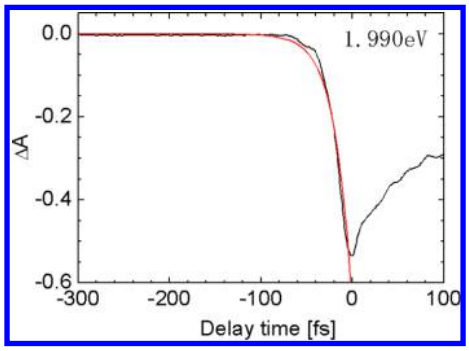

Figure 11. Electronic dephasing time obtained by performing a single-exponential fit (red line) for the ΔA spectra (black line) at 1.990 eV in the negative time region between −314 and −1.1 fs.

Here, by performing a polynomial function fitting with the electronic dephasing time at around the stationary absorption peak, the peak electronic dephasing time, T_2^{ele}, was determined to be 18.30 fs (Figure 12).

CONCLUSION

The ultrafast time-resolved spectroscopy using sub-10 fs pulses for a film of THIATS has been performed in detail. By performing FFT for the ΔA spectrum, the author has observed real-time coherent oscillations due to the vibrational modes in THIATS J-aggregates. Specific vibarational modes were obtained at 285, 485, 555, 824, and 1633 cm^{-1}.

By fitting the real-time traces of ΔA with the sum of two exponential functions and a constant term, the lifetimes of the electronically excited states were found to be $\tau_1 = 52 \pm 5$ fs and $\tau_2 = 540 \pm 78$ fs for the 3-exciton state and 2-exciton state,

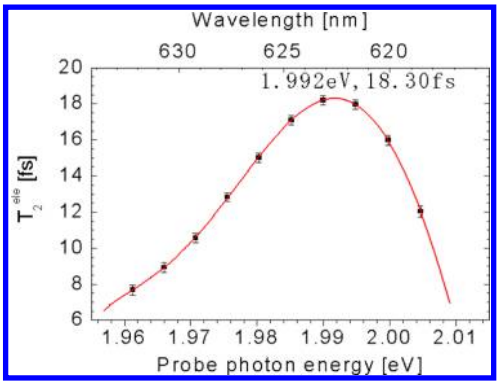

Figure 12. Dependence of the electronic dephasing time on the probe photon energy, obtained by performing a single-exponential fit (black squares with the error bar). By performing a polynomial function fitting (red line) with electric dephasing time, the peak electronic dephasing time T_2^{ele} was determined to be 18.3 fs at 1.992 eV.

respectively. The ΔA values in the negative time range were fitted with the single-exponential functions. As a result, the electronic dephasing time including inhomogeneous decay was determined as T_2^{ele} = 18.3 fs.

It was found that the vibrational mode around 1633 and 824 cm^{-1} is modulated by analyzing the spectrogram. The frequency modulation and the amplitude modulation take place in phase, as shown in the spectrogram analysis. It leads to the conclusion that energy conservation is not satisfied within the single mode but energy flow takes place between the 1633 cm^{-1} mode and the 824 cm^{-1} mode through the low frequency 50 cm^{-1} mode. Such a dynamical modulation of coherent intramolecular vibration in J-aggregates was not previously observed for J-aggregates of pseudoisocyanine (PIC)[14] and tetraphenylporphine tetrasulfonic acid (TPPS).[15−17] The low-frequency mode is presumably assigned to an intermolecular vibrational mode (lattice phonon mode of J-aggregates), which might be coupled to the electronic excitation of delocalized excitons.

APPENDIX

We also tried fitting based on exciton−exciton annihilation dynamics (bimolecular quenching[43]) as follows.

$$\frac{dn}{dt} = -\alpha n - \beta n^2 \quad (1)$$

$$n(t) = \frac{C \exp(-\alpha t)}{1 - \frac{\beta}{\alpha} C \exp(-\alpha t)} \quad (2)$$

$$C = \left(\frac{1}{n(0)} + \frac{\beta}{\alpha}\right)^{-1} \quad (3)$$

$$|\Delta A(t)| = \frac{A \exp(-\alpha t)}{1 - \frac{\beta}{\alpha} A \exp(-\alpha t)} \quad (4)$$

Here, n is the density of the 1-exciton state. Assuming that the transient absorption change reflects the dynamics of the 1-exciton state, the absorption changes spectrally averaged from 1.9 to 1.99 eV (absorption decrease) and from 2.0 to 2.1 eV (absorption increase) are fit by eq 4 with three parameters α, β, and A. The results are shown in Figure 13.

dx.doi.org/10.1021/jp4015228 | J. Phys. Chem. A 2013, 117, 11441−11448

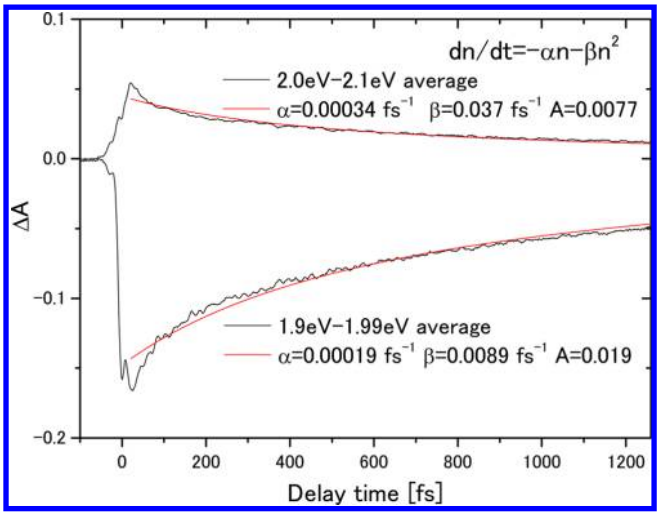

Figure 13. Transent absorption changes averaged from 1.9 to 1.99 eV (absorption decrease) and from 2.0 to 2.1 eV (absorption increase) are fit by eq 4 with three parameters α, β, and A.

The fit is fairly good, demonstrating that the decay times as fast as 52 and 540 fs obtained from the exponential decay fitting are due to exciton−exciton annihilation dynamics. However, a little deviation exists from the fitting curves near zero delay and differences by a factor of 2 or 3 in the fitted parameters α and β This clearly indicates that there is a significant contribution of 2-exciton and 3-exciton states, as known from Figure 2b, such as trimolecular quenching.

AUTHOR INFORMATION

Corresponding Author

*E-mail: kobayashi@ils.uec.ac.jp.

Notes

The authors declare no competing financial interest.

ACKNOWLEDGMENTS

This study was supported by CREST of the Japan Science and Technology Agency, and D.H. would like to thank Mr. Shinpo (Hayashibara, Okayama, Japan) for helpful discussions about the sample.

REFERENCES

(1) Kobayashi, T. *J-Aggregates*; World Scientific: Singapore, 1996.

(2) Kobayashi, T. *J-Aggregates*; World Scientific: Singapore, 2012; Vol. 2.

(3) Kobayashi, T.; Misawa, K. Hierarchical Structure of One-Dimension J-Aggregates. *J. Lumin.* **1997**, *72*−*74*, 38−40.

(4) Kobayashi, T. Hierarchic Structure of J-Aggregates. *Mol. Cryst. Liq. Cryst.* **1996**, *283*, 17−24.

(5) Kobayashi, T. Structure and Nonlinear Properties of Porphyrin J-Aggregates. *Nonlinear Opt.* **1999**, *22*, 301−304.

(6) Misawa, K.; Machida, S.; Horie, K.; Kobayashi, T. Wavelength and Polarization Dependence of Spectral Hole-Burning Efficiency in Highly Oriented J-Aggregates. *Chem. Phys. Lett.* **1995**, *240*, 210−215.

(7) Kobayashi, T. Excitons in J-Aggregates with Hierarchical Structure. *Supramol. Sci.* **1998**, *5*, 343−347.

(8) Minoshima, K.; Taiji, M.; Misawa, K.; Kobayashi, T. Femtosecond Nonlinear Optical Dynamics of Excitons in J-Aggregates. *Chem. Phys. Lett.* **1994**, *218*, 67−72.

(9) Scherer, P. O. J.; Fischer, S. F. On the Theory of Vibronic Structure of Linear Aggregates. Application to Pseudoisocyanin (PIC). *Chem. Phys.* **1984**, *86*, 269−283.

(10) Jelley, E. E. Spectral Absorption and Fluorescence of Dyes in the Molecular State. *Nature* **1936**, *138*, 1009−1010.

(11) Scheibe, G. *Angew. Chem.* **1936**, *49*, 563−563.

(12) Katsumata, T.; Nakata, K.; Ogawa, T.; Koike, K.; Kobayashi, T.; Tokunaga, E. Mechanism for Giant Electrooptic Response of Excitons in Porphyrin J-Aggregates: Molecular Rearrangement Model. *Chem. Phys. Lett.* **2009**, *477*, 150−155.

(13) Bohn, P. W. Aspects of Structure and Energy Transport in Artificial Molecular Assemblies. *Annu. Rev. Phys. Chem.* **1993**, *44*, 37−60.

(14) Nishimura, K.; Tokunaga, E.; Kobayashi, T. Sub-5-fs Two-Dimensional Spectroscopy of Pseudoisocyanine J-Aggregates. *Chem. Phys. Lett.* **2004**, *395*, 114−119.

(15) Kano, H.; Saito, T.; Ueki, A.; Kobayashi, T. First Observation of Dynamic Intensity Borrowing Induced by Coherent Molecular Vibrations in J-Aggregates Revealed by Sub-5-fs Spectroscopy. *Int. J. Mod. Phys. B* **2001**, *15*, 3817−3820.

(16) Kano, H.; Saito, T.; Kobayashi, T. Observation of Herzberg-Teller-Type Wave-Packet Motion in Porphyrin J-Aggregates Studied by Sub-5-fs Spectroscopy. *J. Phys. Chem. A* **2002**, *106*, 3445−3453.

(17) Kano, H.; Saito, T.; Kobayashi, T. Dynamic Intensity Borrowing in Porphyrin J-Aggregates Revealed by Sub-5-fs Spectroscopy. *J. Phys. Chem. B* **2001**, *105*, 413−419.

(18) Lupo, D.; Prass, W.; Scheunemann, U.; Laschewsky, A.; Ringsdorf, H.; Ledoux, I. Second-Harmonic Generation in Langmuir-Blodgett Monolayers of Stilbazium Salt and Phenylhydrazone Dyes. *J. Opt. Soc. Am. B* **1988**, *5*, 300−308.

(19) Rousseau, E.; Koetse, M. M.; Van der Auweraer, M.; De Schryver, F. C. Comparison between J-Aggregates in a Self-Assembled Multilayer and Polymer-Bound J-Aggregates in Solution: a Steady-State and Time-Resolved Spectroscopic Study. *Photochem. Photobiol. Sci.* **2002**, *1*, 395−406.

(20) Gallos, L. K.; Pimenov, A. V.; Scheblykin, I. G.; Van der Auweraer, M.; Hungerford, G.; Varnavsky, O. P.; Vitukhnovsky, A. G.; Argyrakis, P. A Kinetic Model for J-Aggregate Dynamics. *J. Phys. Chem. B* **2000**, *104*, 3918−3923.

(21) Birkan, B.; Gülen, D.; Özçelik, S. Controlled Formation of the Two-Dimensional TTBC J-Aggregates in an Aqueous Solution. *J. Phys. Chem. B* **2006**, *110*, 10805−10813.

(22) Drobizhev, M. A.; Sapozhnikov, M. N.; Scheblykin, I. G.; Varnavsky, O. P.; Van der Auweraer, M.; Vitukhnovsky, A. G. Exciton Dynamics and Trapping in J-Aggregates of Carbocyanine Dyes. *Pure Appl. Opt.* **1996**, *5*, 569−581.

(23) Scheblykin, I. G.; Bataiev, M. M.; Van der Auweraer, M.; Vitukhnovsky, A. G. Dimensionality and Temperature Dependence of the Radiative Lifetime of J-Aggregates with Davydov Splitting of the Exciton Band. *Chem. Phys. Lett.* **2000**, *316*, 37−44.

(24) Scheblykin, I. G.; Sliusarenko, O. Y.; Lepnev, L. S.; Vitukhnovsky, A. G.; Van der Auweraer, M. Excitons in Molecular Aggregates of 3,3′-Bis-[3-sulfopropyl]-5,5′-dichloro-9-ethylthiacarbocyanine (THIATS): Temperature Dependent Properties. *J. Phys. Chem. B* **2001**, *105*, 4636−4646.

(25) Passier, R.; Ritchie, J. P.; Toro, C.; Diaz, C.; Masunov, A. E.; Belfield, K. D.; Hernandez, F. E. Thermally Controlled Preferential Molecular Aggregation State in a Thiacarbocyanine Dye. *J. Chem. Phys.* **2010**, *133*, 134508-1−134508-7.

(26) Noukakis, D.; Van der Auweraer, M.; Toppet, S.; Schryver, F. C. D. Photophysics of a Thiacarbocyanine Dye in Organic Solvents. *J. Phys. Chem.* **1995**, *99*, 11860−11866.

(27) Fukutake, N.; Takasaka, S.; Kobayashi, T. Energy Transfer between Two Kinds of J-Aggregates Studied by Near-Field Absorption-Fluorescence Spectroscopy. *Chem. Phys. Lett.* **2002**, *361*, 42−48.

(28) Shirakawa, A.; Sakane, I.; Kobayashi, T. Pulse-Front-Matched Optical Parametric Amplification for Sub-10-fs Pulse Generation Tunable in the Visible and Near-Infrared. *Opt. Lett.* **1998**, *23*, 1292−1295.

(29) Shirakawa, A.; Sakane, I.; Takasaka, M.; Kobayashi, T. Sub-5-fs Visible Pulse Generation by Pulse-Front-Matched Noncollinear Optical Parametric Amplifier. *Appl. Phys. Lett.* **1999**, *74*, 2268−2270.
(30) Kobayashi, T.; Shirakawa, A. Tunable Visible and Near-Infrared Pulse Generation in a 5 fs Regime. *Appl. Phys. B: Lasers Opt.* **2000**, *70*, S239−246.
(31) Baltuska, A.; Kobayashi, T. Adaptive Shaping of Two-Cycle Visible Pulses Using a Flexible Mirror. *Appl. Phys. B: Lasers Opt.* **2002**, *75*, 427−443.
(32) Baltuska, A.; Fuji, T.; Kobayashi, T. Visible Pulse Compression to 4 fs by Optical Parametric Amplification and Programmable Dispersion Control. *Opt. Lett.* **2002**, *27*, 306−308.
(33) Ishii, N.; Tokunaga, E.; Adachi, S.; Kimura, T.; Matsuda, H.; Kobayashi, T. Optical Frequency and Vibrational Time-Resolved Two-Dimensional Spectroscopy by Real-Time Impulsive Resonant Coherent Raman Scattering in Polydiacetylene. *Phys. Rev. A* **2004**, *70*, 023811-1−023811-7.
(34) Vrakking, M. J. J.; Villeneuve, D. M.; Stolow, A. Observation of Fractional Revivals of a Molecular Wave Packet. *Phys. Rev. A* **1996**, *54*, R37.
(35) Du, J.; Kobayashi, T. Real-Time Observation of Dynamic Coupling between Stretching and Bending Modes in a Polythiophene. *Chem. Phys. Lett.* **2009**, *481*, 204−208.
(36) Kobayashi, T.; Saito, T.; Ohtani, H. Real-Time Spectroscopy of Transition States in Bacteriorhodopsin during Retinal Isomerization. *Nature* **2001**, *414*, 531−534.
(37) Kobayashi, T.; Shirakawa, A.; Matsuzawa, H.; Nakanishi, H. Real-Time Vibrational Mode-Coupling Associated with Ultrafast Geometrical Relaxation in a Polydiacetylene Induced by Sub-5-fs Pulses. *Chem. Phys. Lett.* **2000**, *321*, 385−393.
(38) Kobayashi, T.; Wang., Y.; Wang., Z.; Iwakura, I. Circa Conservation of Vibrational Energy among Three Strongly Coupled Modes of a Cyanine Dye Molecule Studied by Quantum-Beat Spectroscopy with a 7 fs Laser. *Chem. Phys. Lett.* **2008**, *466*, 50−55.
(39) Akins, D, L,; Ozcüelik, S.; Zhu, H.-R.; Guo, C. Fluorescence Decay Kinetics and Structure of Aggregated Tetrakis(*p*-Sulfonatophenyl)Porphyrin. *J. Phys. Chem.* **1996**, *100*, 14390−14396.
(40) Brafman, O.; Lengyel, G.; Mitra, S. S.; Gielisse, P. J.; Plendl, J. N.; Mansur, L. C. Raman Spectra of AlN, Cubic BN and BP. *Solid. State. Commun.* **1968**, *6*, 523−526.
(41) Feldman, D. W.; Parker, J. H., Jr.; Choyke, W. J.; Patrick, L. Phonon Dispersion Curves by Raman Scattering in SiC, Polytypes 3C, 4H, 6H, 15R, and 21R. *Phys. Rev.* **1968**, *173*, 787−793.
(42) Kobayashi, T.; Du, J.; Feng, W.; Yoshino, K. Excited-State Molecular Vibration Observed for a Probe Pulse Preceding the Pump Pulse by Real-Time Optical Spectroscopy. *Phys. Rev. Lett.* **2008**, *101*, 037402.
(43) Kobayashi, T.; Nagakura, S. Bimolecular Quenching of Fluorescence and Interaction between Excited Molecules in Solution. *Mol. Phys.* **1972**, *23*, 1211−1221.